ELSEVIER

Catalysis Today 73 (2002) 83–93

CATALYSIS TODAY

www.elsevier.com/locate/cattod

Alkali and alkaline-earth exchanged faujasites: strength of Lewis base and acid centres and cation site occupancy in Na- and BaY and Na- and BaX zeolites

G. Martra[a,*], R. Ocule[a], L. Marchese[a,b], G. Centi[c], S. Coluccia[a]

[a] *Dipartimento di Chimica IFM, Università di Torino, Via P. Giuria 7, I-10125 Torino, Italy*
[b] *Dipartimento di Scienze e Tecnologie Avanzate, Università del Piemonte Orientale A. Avogadro, C.so Borsalino 54, I-15100 Alessandria, Italy*
[c] *Dipartimento di Chimica Industriale, Università di Messina, Salita Sperone 31, I-98166 Messina, Italy*

Received 9 May 2001; accepted 15 October 2001

Abstract

Sodium and barium forms of X (Si:Al = 1.3) and Y (Si:Al = 3.5) zeolites were studied by IR spectroscopy of adsorbed CO (at low temperature) and CO_2 (at room temperature). In BaY, Ba^{2+} ions substitute almost completely the Na^+ ones at sites S_{II}, and new, stronger Lewis acid sites are formed. In the supercages of X zeolite in sodium form, the Na^+ ions are present at both S_{II} and S_{III} sites. After exchange with Ba^{2+} almost all alkali ions in the supercages are substituted by alkaline-earth ions, which occupy sites S_{II} only. Also, in this case, Ba^{2+} ions behave as stronger Lewis acid centres than Na^+ ions at such sites. However, their Lewis acidity is weaker than for Ba^{2+} species at sites S_{II} in Y zeolite, because of the lower Si:Al ratio.

IR spectra of adsorbed CO_2 revealed that the Lewis basicity of the framework oxygen atoms of NaX, put in evidence by the formation of carbonate-like species, is strongly decreased by exchanging Na^+ with Ba^{2+}, as in BaX CO_2 is linearly polarised on the cations only. Calculation of the partial negative charge on the framework oxygens (carried out on the basis of the Sanderson's electronegativity equalisation method) confirmed this effect for X systems, and indicated that the exchange of Na^+ with Ba^{2+} resulted in a decrease in basicity in the case of Y zeolite also, (which even in the sodium form was unable to give rise to carbonate-like species by interaction with CO_2).

Keywords: Na^+ and Ba^{2+} X and Y zeolites; IR spectroscopy of adsorbed CO and CO_2

---

1. Introduction

Zeolites and related microporous materials have found a widespread use in several technological fields. They act as efficient heterogeneous catalysts, as adsorbents, and as molecular sieves in gas separation processes, to name only a few major applications. Such a broad spectrum of uses results from the possibility to tune the structure of these materials to each particular application by choosing zeolites with cavities and/or channels of due shape and dimension, and by introducing appropriate active centres within the pores. Indeed, isomorphic substitution of tetrahedrally coordinated silicon with aluminium atoms generates a negative charge on the oxygens of the framework. The compensation of these charges requires the presence of countercations. These last species can be easily exchanged, which enables the

---

[*] Corresponding author. Tel.: +39-11-670-7538; fax: +39-11-670-7855.
E-mail address: martra@ch.unito.it (G. Martra).

PII: S0920-5861(01)00521-1

introduction of the most useful centres for the envisaged application.

As for heterogeneous catalysis, the exchange with ammonium ions and subsequent calcination results in the production of Brønsted acid materials. These are the most widely investigated zeolitic systems by far, as they are employed in the petrochemical industry, and a number of review articles and monographs dealing with this subject have been published [1–5].

Zeolites containing transition metal ions, as countercations or even in the framework, represent another class of widely studied microporous materials [6], owing to their actual or potential use as catalysts in environmentally benign processes (e.g. selective oxidations producing a lower amount of waste, pollutant abatement).

On the other hand, there is less information on basic sites in zeolites, recently reviewed by Barthomeuf [7]. Typically, basic properties exist in zeolites with alkali metal cations compensating for the negative charge on the framework [8,9]. The presence of the alkali cations enhances the electron density of the framework oxygen, which can act as basic sites. The strength of these centres depends on the structure of the framework, on its chemical composition and on the nature of the countercations [7].

Synthetic zeolites exchanged with alkaline-earth cations received even less attention. This may be due to the fact that during the activation of these materials by dehydration at high temperature, dissociation of water molecules adsorbed on the countercations can occur. This process results in the formation of both Brønsted acid and base sites [10], and their simultaneous presence can then result in a loss of selectivity in catalytic applications.

However, alkaline-earth exchanged zeolites, in particular BaY, have recently been reported as constrained media for photoassisted selective oxidation of hydrocarbons with O_2 under irradiation with visible light (instead of UV) [11,12]. Alkaline-earth exchanged zeolites were found to be more efficient in this process than alkali exchanged zeolites, and this fact was attributed to the higher positive field of the divalent cations, resulting in a higher stabilisation of the polar charge-transfer states of hydrocarbon–oxygen collisional pairs.

Furthermore, BaY zeolites have been reported to exhibit interesting properties as adsorbing materials in selective NO_x recirculation (SNR) proposed for the abatement of such pollutants in lean exhaust gases [13].

The rationalisation of the behaviour of these materials, which is the basis for the design of new systems, needs a detailed understanding of the nature and structure, and consequently of the physico-chemical properties of the sites within their cavities.

In this work, a study of the Lewis acid and base centres and cation site occupation in barium-exchanged faujasites, carried out by infrared spectroscopy of adsorbed CO and CO_2 as probe molecules, is reported.

Two different types of faujasites were investigated, viz. zeolites X and Y, in order to evaluate the influence of the Si:Al ratio. The parent sodium forms of both zeolites was studied as well, to elucidate the effect of the exchange of Na^+ by Ba^{2+} ions.

2. Experimental

Commercial NaY (Linde, Si:Al = 3.5) and NaX (Union Carbide, Si:Al = 1.3) zeolites were employed. From these samples, barium containing forms were prepared via ion exchange, by stirring in a solution of $Ba(CH_3COO)_2$ at 343 K for 8 h, followed by filtering and washing with distilled water. This procedure was repeated twice more, resulting in the attainment of the maximum level of exchange of Na^+ with Ba^{2+} determined by atomic absorption spectroscopy. Indeed, it was found that a further repetition of the procedure did not result in an increase of the Ba^{2+}/Na^+ ratio. The exchanged samples were then dried at 383 K for 3 h and calcined at 823 K for 3 h in air. The compositions of the samples and their codes are listed in Table 1. Although the exchange of Na^+ with Ba^{2+} was not complete, for the sake of simplicity the sam-

Table 1
Codes and composition of the zeolite samples

Code	Composition
NaY	$Na_{43}Al_{43}Si_{149}O_{384}$
BaY	$Ba_{15}Na_{13}Al_{43}Si_{149}O_{384}$
NaX	$Na_{83}Al_{83}Si_{109}O_{384}$
BaX	$Ba_{22}Na_{39}Al_{83}Si_{109}O_{384}$

Table 2
Electronegativity data (S) of the elements in the zeolite samples used for the calculation of the partial charge on framework oxygen atoms at sites S_{II} (from [14])

Element	S
O	5.21
Na	0.70
Si	2.84
Al	2.22
Ba	0.78

ples containing barium will be referred to as BaY and BaX.

In Table 2 the electronegativity data (from [14]) used for the calculation of the partial negative charge of framework oxygen atoms at S_{II} sites are reported.

For the IR measurements, powders were pressed into self-supporting pellets of 10–15 mg cm^{-2} and placed inside an IR cell which allowed in situ high-temperature treatments, gas dosage, room and low-temperature measurements to be made, permanently connected to a conventional vacuum line (residual pressure, 1.33×10^{-4} Pa). The zeolite pellets were heated under vacuum up to 623 K (1 K min^{-1}), and then outgassed at this temperature for 1 h. The slow heating rate prevented the dissociation of the water molecules adsorbed on divalent cations. IR spectra of adsorbed NH_3 (not reported) indicated that no Brønsted acid centres were present in BaY, while BaX contained the same small amount of protons already present in the parent NaX zeolite [15].

For the low temperature measurements, although the IR cell was permanently cooled with liquid nitrogen, the actual sample temperature was likely to be ca. 100–110 K.

The IR spectra (resolution, 2 cm^{-1}) were recorded on a IFS48 Bruker Fourier transform spectrometer, equipped with a MCT detector. All spectra are reported in absorbance, the background spectrum of the samples before gas adsorption being subtracted.

High purity CO (UCAR) and CO_2 (Praxair) were employed. CO was used without any further purification, except liquid nitrogen trapping, while CO_2 was used after several freeze-pump-thaw cycles.

3. Results and discussion

3.1. Monitoring acid sites: IR spectra of CO adsorbed at low temperature on NaY and BaY

As recently reviewed by Knözinger and Huber [16], IR spectroscopy of adsorbed CO is a useful tool to obtain information on the Lewis acid strength of charge-balancing metal cations in zeolites. Indeed, the CO frequency shift induced by adsorption is highly sensitive to the electric field strength produced by these cations, which depends on the sites where they are located and on their charge/size ratio. For the sake of clarity, the different extra-framework sites which may allocate cations in a faujasite-type structure are indicated in Scheme 1 by different symbols and by conventional lettering.

3.1.1. CO on NaY

The spectra of CO adsorbed under decreasing equilibrium pressure on NaY at 100–110 K are shown in Fig. 1. At high coverage a very intense band in the 2180–2160 cm^{-1} range (maximum out of scale in the figure) and a peak at 2140 cm^{-1}, with a shoulder on the low frequency side, were present (Fig. 1, curve a). By progressively decreasing the CO equilibrium pressure, all these components decreased in intensity (Fig. 1, curves b–v), but differences in their behaviour in dependence on the CO coverage were observed. In fact, the main band at 2180–2160 cm^{-1} underwent a progressive narrowing towards high frequency, resulting

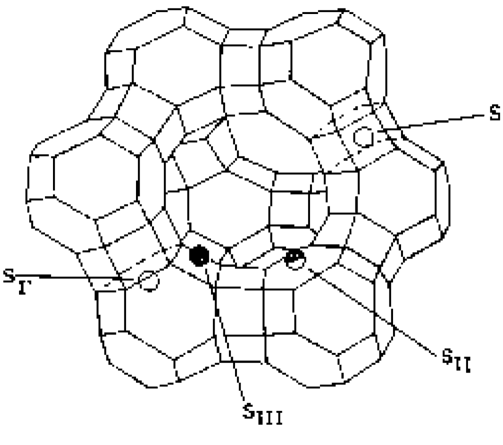

Scheme 1.

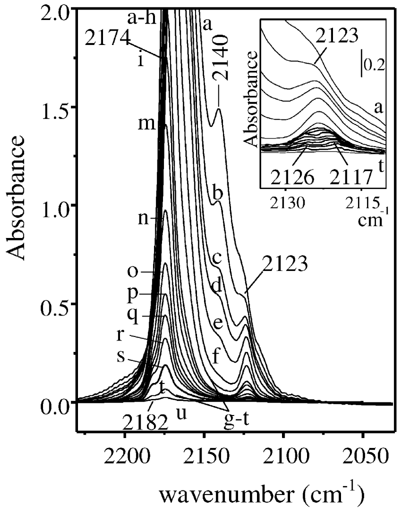

Fig. 1. IR spectra of CO adsorbed at low temperature (100–110 K) on NaY preoutgassed at 623 K for 1 h. Curves a–u are spectra taken at decreasing CO equilibrium pressure, from (a) 6.66×10^3 to (u) 0.66 Pa CO.

in a defined peak at 2174 cm^{-1} (Fig. 1, curve i), while the peak at 2140 cm^{-1} vanished for intermediate CO coverage, allowing the low frequency component to be observed as a well defined peak at 2123 cm^{-1} (Fig. 1, curve f). This component initially appeared as a narrow peak, but by decreasing the amount of adsorbed CO it shifted to lower frequency and became broader, finally appearing as the superposition of two components located at 2126 and 2117 cm^{-1}.

On the basis of well established literature on the IR spectroscopy of probe molecules adsorbed in zeolites, recently reviewed by Knözinger and Huber [16] and Coluccia et al. [17], the band at 2140 cm^{-1} is assigned to CO in a liquid-like phase formed at relatively high equilibrium pressure inside the zeolite cavities, while the peak in the 2180–2160 cm^{-1} range, shifted to higher frequency as compared to free CO (2143 cm^{-1}), corresponds to CO polarised through the C-end on Na^+ cations in S_{II} sites. These are the only sites populated in the supercages and then accessible to CO, which, in contrast, cannot enter sodalite cages and hexagonal prisms, where the S'_I and S_I sites, respectively, are located. The progressive narrowing and shift to higher frequency exhibited by this band upon decreasing the amount of adsorbed CO suggests that more complex species are formed at high CO coverage, as commented on in the following.

At very low coverage a very weak component at 2182 cm^{-1} was revealed. This signal is assigned to CO adsorbed on Na^+ ions hosted in a minor fraction of S_{II} sites constituted by hexagonal rings (T_6O_6; T = Si, Al) containing one Al atoms, while the most common ones, hosting Na^+ ions on which are adsorbed CO molecules responsible for the main band at 2174 cm^{-1}, contain two Al atoms [16]. It can be assumed that the higher the number of Al atoms in a S_{II} ring, the larger the negative charge density on the oxygen atoms in it, which decreases the positive electric field of the hosted Na^+ ion. This results in a lower frequency of the band due to adsorbed CO.

As for the minor component at 2123 cm^{-1}, its behaviour suggests that it is due to species which undergo some transformation in dependence of the amount of CO adsorbed in the zeolite cavities. For the sake of clarity, it is better to analyse the spectral features observed from low to high CO coverage. At low CO coverage, two ill resolved components at ca. 2126 and 2117 cm^{-1} are present. On the basis of the ratio between the reduced masses of ^{12}CO and ^{13}CO oscillators and the natural $^{12}C/^{13}C$ distribution, the high frequency component should correspond to the ^{13}CO counterpart of the peak observed for these levels of CO coverage at 2174 cm^{-1}, while, on the basis of recent experimental results [18] and quantum chemical calculations [19,20], the band at 2117 cm^{-1} can be assigned to Na^+–$O^{12}C$ adducts, where the CO molecules are coordinated on the Na^+ ion through the oxygen end. As reported for similar spectral features observed for a Na-ETS-10 system [21], the evolution of these two components by increasing the amount of adsorbed CO can be ascribed to the formation of $Na^+(^{13}CO)(^{12}CO)$ and $Na^+(O^{12}C)(^{12}CO)$ dicarbonylic species, both contributing to the 2123 cm^{-1} band. In fact, a $Na^+(^{13}CO)(^{12}CO)$ dicarbonyl is expected to absorb at lower frequency with respect to a $Na^+(^{13}CO)$ monocarbonyl, while a $Na^+(O^{12}C)(^{12}CO)$ adduct should absorb at higher frequency than a $Na^+(O^{12}C)$ one. Thus, the analysis of these minor features allowed to recognise the formation of dicarbonylic adducts on Na^+ ions at high CO coverage. Of course, the same conversion between mono- and dicarbonylic adducts on Na^+ ions should occur for ^{12}CO molecules C-end coordinated to the

Na^+ ions, which are responsible for the main band at 2180–2160 cm^{-1}. In this case, the addition on a second ^{12}CO molecule to a Na^+–^{12}CO species (producing the narrow peak at 2174 cm^{-1}) should result in a decrease of the frequency of the CO stretching absorption. Owing to the outstanding intensity of the band at 2180–2160 cm^{-1}, exceeding the high detection limit of the spectrometer, it was not possible to observe the spectral features related to this process, which should be responsible for the shift broadening towards low frequency exhibited by the detectable part of this absorption upon increasing CO coverage.

3.1.2. CO on BaY

The same CO adsorption experiment was performed on the BaY sample, recording IR spectra at decreasing CO coverage. Spectral features similar to those obtained for the NaY system were observed, with some significant differences in position and relative intensity. In particular, the main band due to CO adsorbed on cations appeared shifted to higher frequency (Fig. 2, curve a), and at medium-low level of CO coverage a peak at 2181 cm^{-1}, with a weak shoulder at ca. 2172 cm^{-1} was observed (Fig. 2, curve p). Ba^{2+} ions, having a charge (Z^{n+}) to radius (r) ratio ($Z^{n+}/r = 1.48$) higher than Na^+ ions ($Z^{n+}/r = 1.05$), produce a stronger positive electric field, and this should result in a higher stretching frequency of adsorbed CO [22–24]. On this basis, the 2181 cm^{-1} band can be assigned to Ba^{2+}–(^{12}CO) species, and the shoulder at ca. 2172 cm^{-1} to CO adsorbed on unexchanged Na^+ ions still present in the supercages. The low intensity of this component indicates that almost all Na^+ ions in site S_{II}, accessible to CO, have been substituted by Ba^{2+} species.

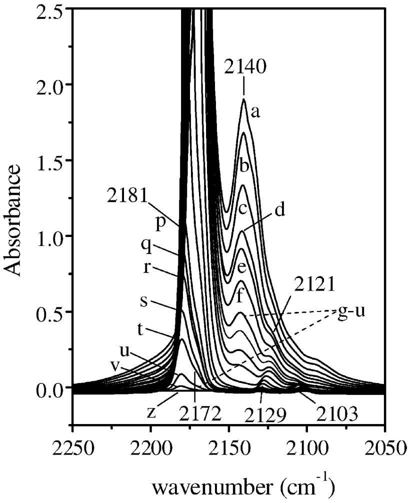

Fig. 2. IR spectra of CO adsorbed at low temperature (100–110 K) on BaY pre-outgassed at 623 K for 1 h. Curves a–z are spectra taken at decreasing CO equilibrium pressure, from (a) 6.66×10^3 to (z) 0.66 Pa CO.

As in the case of the NaY sample, the band due to CO C-end adsorbed on cations exhibited a minor counterpart at lower frequency. However, for the BaY zeolite it appeared significantly less intense than for the NaY system, simply producing, at high CO coverage, a weak and ill resolved shoulder at ca. 2121 cm^{-1}, which is converted in components at 2129 and 2103 cm^{-1} at low CO coverage. The weaker intensity of this signal can be easily rationalised taking into account that each Ba^{2+} ion substituted two Na^+ ions, thus the BaY sample contains a significant lower amount of cations (one half, theoretically). Nevertheless, the amount of Ba^{2+} ions in supercages must be large enough to produce the intense band at 2180–2160 cm^{-1} due to C-end carbonylic adducts adsorbed on such sites. The conversion of the 2121 cm^{-1} component in the two signals at 2129 and 2103 cm^{-1} by decreasing the CO coverage parallels that exhibited by the 2123 cm^{-1} component in the NaY sample. Also in this case, under decreasing CO coverage the conversion of $Ba^{2+}(^{13}CO)(^{12}CO)$ and $Ba^{2+}(O^{12}C)(^{12}CO)$ species (shoulder at 2121 cm^{-1}) to $Ba^{2+}(^{13}CO)$ (component at 2129 cm^{-1}) and $Ba^{2+}(O^{12}C)$ (component at 2103 cm^{-1}) occurred.

In conclusion, the comparison between the spectra of CO adsorbed at low temperature on NaY and BaY zeolites evidences that the extensive exchange of Na^+ with Ba^{2+}ions resulted in a significant decrease of the number of cations exposed in the supercages, which, on the other hand, behave as stronger Lewis acid centres.

3.2. Monitoring acid sites: IR spectra of CO adsorbed at low temperature on NaX and BaX

3.2.1. CO on NaX

A similar investigation was carried out on high Al content zeolites. The spectrum of NaX recorded at high CO coverage exhibited a main component at

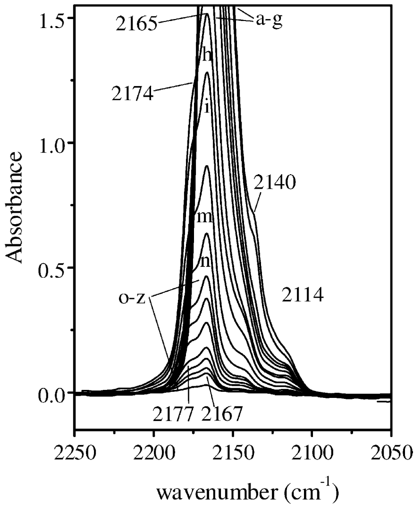

Fig. 3. IR spectra of CO adsorbed at low temperature (100–110 K) on NaX pre-outgassed at 623 K for 1 h. Curves a–z are spectra taken at decreasing CO equilibrium pressure, from (a) 6.66×10^3 to (z) 0.66 Pa CO.

2160–2145 cm^{-1}, so strong in intensity that it completely absorbs the IR light in that region. However, two shoulders at 2140 and 2114 cm^{-1} can be recognised (Fig. 3, curve a).

By decreasing the CO coverage, the main band at 2160–2145 cm^{-1} decreased in intensity and underwent a narrowing toward high frequency (Fig. 3, curves b–g), so that a peak at 2165 cm^{-1} became detectable (Fig. 3, curve h). Noticeably, a new shoulder at 2174 cm^{-1} appeared. By further decreasing the amount of adsorbed CO, these two components progressively decreased in intensity, with a slight change in their relative intensity, in favour of the absorption at 2174 cm^{-1} (Fig. 3, curves i–z). As in the cases of Na- and BaY zeolites, the dominant band, located at a frequency higher than the absorption of free CO, must be assigned to CO polarised through the C-end on cations exposed in the supercages. By analogy with the case of Na- and BaY, at high CO coverage this band is associated with dicarbonylic adducts, which, by decreasing the amount of adsorbed CO, are transformed in monocarbonylic ones, responsible for the two components at 2165 and 2174 cm^{-1}. The presence of two monocarbonylic bands indicates that two types of Na^+ ions able to polarise CO are exposed in the supercages. Indeed, structural data evidenced that, besides S_{II} sites, a fraction of S_{III} sites is also occupied by cations in NaX zeolites [25], as a higher number of countercations is needed to compensate for the larger negative charge generated by a higher level of substitution of silicon with aluminium atoms. In sites S_{III}, located slightly about four-membered rings, cations are surrounded by four oxygen atoms, while, as reported above, in sites S_{II} they are hosted in hexagonal rings, where six oxygen atoms are present. Na^+ ions in the two extraframework positions exhibit a different electric field, decreasing as the number of neighbouring oxygen atoms, providing a compensating negative charge, increases. The CO stretching frequency of molecules adsorbed on positively charged sites with the carbon pointing towards the cation increases with respect to free CO (hypsochromic shift) as the strength of the positive field increases. According to a previous study [26], the absorption at 2164 cm^{-1} can be assigned to CO molecules coordinated to Na^+ ions at S_{II} sites, while the component at 2175 cm^{-1}, weaker in intensity and shifted to higher frequency, can be ascribed to CO adsorbed on Na^+ ions at S_{III} sites. The lower intensity of the latter indicates that S_{III} positions are less populated than S_{II}.

The influence of the neighbouring oxygen atoms can account also for the difference between the stretching frequency of CO adsorbed on Na^+ ions at S_{II} in NaY (2172 cm^{-1}) and NaX (2165 cm^{-1}) zeolites. In both cases cations are surrounded by the same number of framework oxygen, but in NaX these atoms bear a higher electron density, due to the lower Si:Al ratio [27,28]. This results in a larger shielding of the positive electric field in the proximity of the cation, and, consequently, in a lower hypsochromic shift of the stretching vibration of CO molecules coordinated to Na^+ ions.

Interestingly, the component at 2140 cm^{-1}, due to CO weakly adsorbed in a liquid-like phase at relatively high equilibrium pressure, appeared significantly less intense with respect to the main cation-specific band at higher frequency if compared with the corresponding spectra obtained for the NaY sample (Fig. 1). This could be another consequence of the higher population of cationic sites in the supercages of the NaX systems, leaving a reduced volume available to CO in such weakly physisorbed form.

The minor feature at 2114 cm^{-1} exhibited a dependence on the CO coverage similar to that observed for the Na- and BaY samples, and then it can be ascribed to CO molecules coordinated to the cations through their O atom, passing from dicarbonylic to monocarbonylic species as the amount of adsorbed CO decreases. Noticeably, the relative intensity of this component appeared lower for the NaX zeolite than for the NaY one, suggesting that the higher population of cationic sites in the supercages affected also the equilibrium between the adsorption of CO molecules through their C- or O-end.

3.2.2. *CO on BaX*

As for the BaX sample, the overall spectral pattern observed at high CO coverage is characterised by a quite narrow main band in the 2170–2155 cm^{-1} range of intensity exceeding the high detection limit, and by two well-resolved components at 2140 and 2114 cm^{-1}, the last with an evident shoulder at 2117 cm^{-1} (Fig. 4, curve a). These two components exhibited a higher relative intensity than in the case of the NaX system (Fig. 3, curve a).

When the CO coverage was decreased enough to allow the intensity of the main band to fall below the high detection limit, the peak was at 2172 cm^{-1}, with a weak shoulder at 2177 cm^{-1} (Fig. 4, curve p). This minor feature corresponds to the high frequency component observed in the spectrum of the parent NaX sample at low CO coverage (Fig. 3, curves o–z), and can be assigned to CO molecules C-end coordinated to Na$^+$ ions at S$_{\mathrm{III}}$ sites. However, its very weak intensity indicates that only few Na$^+$ ions are left in such positions by exchange with Ba^{2+} ions. In contrast, the peak at 2172 cm^{-1} is specific for the BaX zeolite, and can be ascribed to CO molecules C-end coordinated to Ba^{2+} ions exposed in the supercages. As reported above, the charge to radius ratio is higher for Ba^{2+} than for Na$^+$; thus, the stretching mode of CO molecules polarised through the C-end on the alkaline-earth cations should absorb at higher frequency with respect to those interacting with the alkali ones, located in the same type of site in the supercages, as resulted from the comparison of the spectra of CO adsorbed on NaY and BaY also. On this basis, it can be proposed that the peak at 2172 cm^{-1}, higher in frequency than the component observed at 2165 cm^{-1} in the case of the NaX sample, is assigned to CO molecules C-end coordinated to Ba^{2+} ions at S$_{\mathrm{II}}$ sites. No traces of the 2165 cm^{-1} band, due to analogous CO adducts on Na$^+$ ions at this type of sites, were observed, indicating that all Na$^+$ ions present in sites S$_{\mathrm{II}}$ in the parent sodium form were exchanged with Ba^{2+} ions.

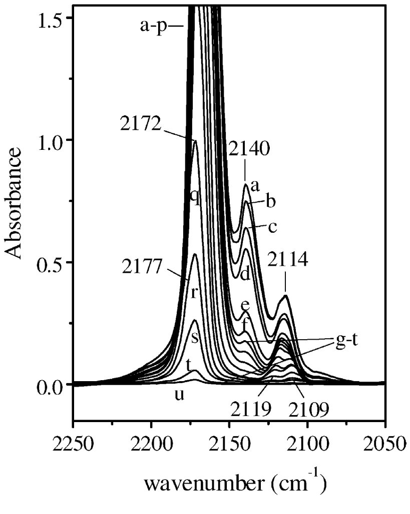

Fig. 4. IR spectra of CO adsorbed at low temperature (100–110 K) on BaX pre-outgassed at 623 K for 1 h. Curves a–u are spectra taken at decreasing CO equilibrium pressure, from (a) 6.66×10^3 to (u) 0.66 Pa CO.

Furthermore, it can be noticed that the 2172 cm^{-1} peak appears located at lower frequency with respect to the band due to CO adsorbed on Ba^{2+} ions at S$_{\mathrm{II}}$ sites in BaY, observed at 2181 cm^{-1} (Fig. 3). As commented above for CO adsorbed on Na$^+$ ions at this type of sites in Y and X matrices, this difference results from the higher compensating negative charge provided by the oxygen atoms of the framework of the X zeolite.

Sites S$_{\mathrm{III}}$ are not populated by Ba^{2+} ions, as absorptions higher in frequency then the weak shoulder at 2177 cm^{-1}, due to CO molecules polarised on Na$^+$ at such sites, were not observed. This fact can be rationalised by taking into consideration that each Ba^{2+} ion replaced two Na$^+$ ions, and then a lower number of cationic sites must be populated to counterbalance the negative charge of the frame. Apparently, S$_{\mathrm{II}}$ sites are in a number higher enough to host all Ba^{2+} exposed in the supercages, and then these ions preferentially populate this type of sites, where they can be stabilised by six framework oxygen atoms.

The decrease of the amount of cations exposed in the supercages should be responsible of the higher relative intensity of the component at 2140 cm^{-1}, due to CO in a liquid-like phase, as more space if left available for the intake of CO in this form.

The 2114 cm^{-1} component is associated with CO stabilised through the O-end, as described for the other samples, and generates two distinct features at 2119 and 2109 cm^{-1} by decreasing the CO coverage. Based on the comments reported above, the first absorption is the ^{13}CO counterpart of the peak at 2181 cm^{-1}, while the second one is assigned to Ba^{2+} (O^{12}C) adducts. Noticeably, this last component appeared at a frequency higher than the analogous signal observed for the BaY sample, located at 2103 cm^{-1}, as the bathochromic shift of the stretching mode of CO molecules O-end coordinated to positively charged sites decreases as the strength of the positive field decreases [23].

3.3. Monitoring base sites: IR spectra of CO_2 adsorbed at room temperature on Na^+ and Ba^{2+} zeolites

The variations of the Lewis acid properties upon cation exchange have been thoroughly described in the previous sections. However, cation exchange modifies the properties of framework oxygen atoms also, which can act as Lewis base sites [7]. Based on this fact, an IR study of the adsorption of CO_2 was carried out, in order to evaluate the effect of the exchange of Na$^+$ with Ba^{2+} ions on the Lewis basic feature of the framework of the systems considered.

In fact, CO_2 is frequently employed to probe the Lewis acid sites of both metal oxides [29,30] and zeolites [31], as it can interact with cations in low coordination. However, being amphoteric in nature, it is sensitive to basic centres (oxygen anions) adjacent to the cations.

Fig. 5 shows the IR spectra in the 2400–1300 cm^{-1} range of CO_2 adsorbed on NaX zeolite. A main band at 2355 cm^{-1} is observed, while at lower frequency two pairs of bands at 1710 and 1360 cm^{-1} and at 1485 and 1430 cm^{-1} are produced. As discussed in detail in previous work [15], the main peak at 2355 cm^{-1} is due to the asymmetric stretching (ν_3 mode) of CO_2 molecules linearly coordinated to Na$^+$ cations (with a weak satellite at 2287 cm^{-1} due to the $^{13}CO_2$ counterpart), while the two couples of bands at lower frequency are due to the symmetric and asymmetric stretching modes of polydentate (species A, bands at 1485 and 1430 cm^{-1}) and monodentate (species B, bands at 1710 and 1360 cm^{-1}) carbonate-like groups. The presence of such species clearly indicates that the framework of the NaX zeolites contains oxygen atoms basic enough to develop a nucleophylic attack to CO_2 molecules. However, the presence of linearly

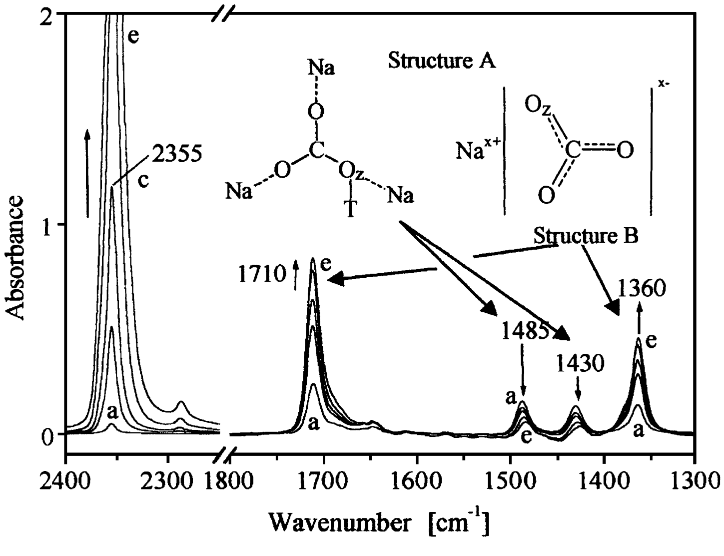

Fig. 5. IR spectra of CO_2 adsorbed at room temperature under increasing pressure on NaX pre-outgassed at 623 K for 1 h. CO_2 equilibrium pressure varies from (a) 1.33 to (e) 2.66 × 10^3 Pa.

adsorbed CO_2 suggests that not all Na^+ ions in the supercages are surrounded by so basic oxygens.

Nevertheless, at low CO_2 coverage these cationic sites can be involved in the stabilisation of carbonate-like species also, and polydentate species A prevail (Fig. 5, curve a). Competition for Na^+ cations can occur at higher CO_2 coverage, and carbonate species are converted into less symmetric species B (Fig. 5, b–e), which accommodate a larger number of carbonate groups in the supercages.

Conversely, by adsorbing CO_2 on BaX zeolite no traces of the pairs of bands due to mono- or polydentate carbonate-like groups were observed, and the spectrum appeared dominated by a peak at 2358 cm^{-1} with a minor satellite at 2290 cm^{-1} and two very weak partners at 1380 and 1270 cm^{-1}, all components progressively increasing in intensity by dosing further CO_2 (Fig. 6). This spectral pattern corresponds to that observed for CO_2 molecules linearly coordinated to cations in faujasites [32]. The bands at 2258 and 2290 cm^{-1} can be assigned to the ν_3 mode of $^{12}CO_2$ and $^{13}CO_2$ molecules adsorbed on Ba^{2+} ions, respectively. Noticeably, they are located at higher frequency with respect to the analogous components observed for the NaX sample. As the hypsochromic shift of the to ν_3 band of linearly adsorbed CO_2 molecules from the 2343 cm^{-1} value corresponding to free CO_2 molecules increases as the strength of the positive field of cationic adsorbing sites increases [33], this feature provides a confirmatory evidence of the higher strength of the positive field of Ba^{2+} with respect to Na^+ ions in the supercages of X zeolites, already put in evidence by the IR spectra of CO adsorbed at low temperature. The very weak components at 1380 and 1270 cm^{-1} can be attributed to the Fermi-resonant vibrations ($2\nu_2$ overtone and ν_1 symmetric stretching modes), which are IR forbidden in gas phase, but become partly IR activated for molecules polarised on cations [32].

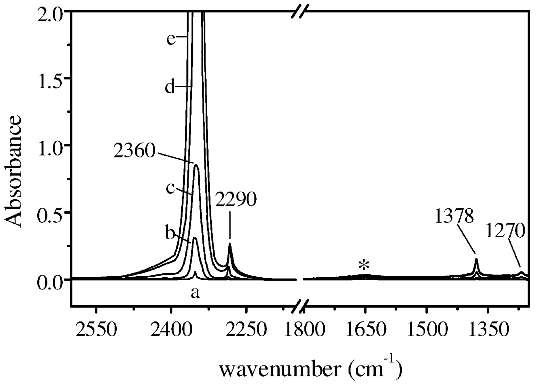

Fig. 6. IR spectra of CO_2 adsorbed at room temperature under increasing pressure on BaX pre-outgassed at 623 K for 1 h. CO_2 equilibrium pressure varies from (a) 1.33 to (e) 2.66×10^3 Pa.

The absence of bands due to carbonate-like groups indicated that framework oxygen atoms surrounding the cations in BaX behave as weaker basic centres. Systematic studies on zeolites exchanged with different kind of cations, recently reviewed by Barthomeuf [7], indicated that the basicity of zeolites depends, for a given structure, on the electronegativity of the countercations, which influences the amount of negative charge on the framework oxygen atoms.

According to the electronegativity equivalence method (EEM) [34], the partial charge on the framework oxygens can be calculated. Such calculation was carried out for the oxygen atoms at S_{II} sites in the X faujasites, where both Ba^{2+} and Na^+ ions were supposed to be located on the basis of the IR spectra of adsorbed CO, by using the formula proposed for this type of site by Huang and Kaliaguine [35]. By assuming the electronegativity values reported in Table 2, a partial negative charge of oxygen atoms at S_{II} sites, $\delta_O = -0.413$ was obtained for NaX, while a value $\delta_O = -0.330$ was calculated for BaX, in good agreement with previous data reported in the literature [14,35]. These results well account for the lower basic strength of framework oxygen atoms adjacent to Ba^{2+} ions at sites S_{II} in BaX zeolite.

CO_2 adsorption was carried out on NaY and BaY also. In both cases, only bands due to CO_2 molecules linearly polarised on cations were observed, whereas no signals related to the formation of carbonate species were detected (spectra not reported for the sake of brevity). In Y zeolite a lower amount of silicon is isomorphically substituted with aluminium atoms, and then a lower negative charge is generated on the framework oxygens. The Lewis basic character of these atoms is then quite weak, and they cannot act as nucleophylic agents towards CO_2 molecules. Due to this absence of reactivity, CO_2 was a “silent” probe to test possible differences in the basic features of framework oxygens of NaY and BaY. However, the partial negative charge on oxygen atoms at S_{II} sites was calculated in the two cases. Values $\delta_O = -0.340$ and

$\delta_O = -0.310$ were obtained for NaY and BaY respectively, indicating that also in the case of Y zeolites the Lewis basic character of framework oxygen adjacent cations at S_{II} sites is decreased by exchanging Na^+ with Ba^{2+} ions.

4. Conclusions

The study by IR spectroscopy of adsorbed CO and CO_2 allowed to monitor the features of Lewis acid and base sites in the supercages of Y and X zeolites exchanged with Na^+ and Ba^{2+} ions. As a common features, in all cases evidence of the formation at high CO coverage of dicarbonylic adducts polarised on the cations were obtained.

The comparison between the frequency of monocarbonylic species formed at low CO coverage indicated that Ba^{2+} ions, located at sites S_{II} in both Y and X zeolites, exhibit a higher Lewis acid strength than Na^+ ions hosted in the same type of sites, owing to their higher charge to radius ratio.

Furthermore, the Lewis acidity of both Ba^{2+} and Na^+ ions appeared dependent upon on the aluminium content of the zeolite framework, which generates a different amount of negative charge on the framework oxygen, resulting in a difference in the decrease of the positive electric field in proximity of the cationic sites.

However, the amount of negative charge on framework oxygen was affected by the exchange of Na^+ with Ba^{2+} ions also. In fact, the substitution of alkali with alkaline-earth cations resulted in the loss of basic reactivity of framework oxygen of X zeolite towards adsorbed CO_2 molecules. A decrease of the partial negative charge of oxygen atoms adjacent Ba^{2+} ions with respect to those surrounding Na^+ ions was calculated for Y zeolite also, on the basis of the Sanderson's electronegativity model. Such decrease results from the higher electronegativity of Ba^{2+} ions with respect the Na^+ ones.

In NaY, BaY and BaX, where supercages are less crowded by cations with respect to NaX, more space is left available to intake CO in a liquid-like form at relatively high pressure. Furthermore, also the equilibrium between the two coordination mode of CO molecules on cations, through the C- or the O-end, appeared dependent on the amount of cations at sites in the supercages.

Acknowledgements

Financial support from MURST (Cofin 98 Area 03) and CNR (PF Materiali speciali) is gratefully acknowledged.

References

[1] L. Forni, Catal. Rev. Sci. Eng. 8 (1974) 65.
[2] H.A. Benesi, B.H.C. Winquist, Adv. Catal. 27 (1978) 99.
[3] H.-P. Böhm, H. Knözinger, in: J.R.A. Anderson, M. Boudart (Eds.), Catalysis Science and Technology, Vol. 4, Springer, Berlin, 1983, p. 39.
[4] R.A. van Santen, G.J. Kramer, Chem. Rev. 95 (1995) 637.
[5] A. Zecchina, C. Otero Areán, Chem. Soc. Rev., 1996, 187.
[6] A. Corma, Chem. Rev. 95 (1995) 559.
[7] D. Barthomeuf, Cat. Rev. Sci. Eng. 38 (1996) 521.
[8] D. Barthomeuf, A. de Mallmann, in: P.J. Grobet, W.J. Mortier, E.F. Vansant, G. Schulz-Ekloff (Eds.), Innovation in Zeolite Materials Science, Studies in Surface Science and Catalysis, Vol. 37, Elsevier, Amsterdam, 1988, p. 356.
[9] D. Barthomeuf, G. Coudurier, J.C. Vedrine, Mater. Chem. Phys. 18 (1988) 553.
[10] D. Barthomeuf, C. Mirodatos, J.C. Vedrine, J. Phys. Chem. 92 (1988) 1637.
[11] F. Blatter, F. Moreau, H. Frei, J. Phys. Chem. 98 (1994) 13403.
[12] F. Blatter, H. Sun, H. Frei, Chem. Eur. J. 2 (1996) 385;
F. Blatter, H. Sun, H. Frei, Angew. Chem. Int. Ed. Engl. 35 (1996) 635.
[13] O. Monticelli, R. Loenders, P.A. Jacobs, J.A. Martens, Appl. Catal. B: Environ. 21 (1999) 215.
[14] W.J. Mortier, J. Catal. 55 (1978) 138.
[15] G. Martra, S. Coluccia, P. Davit, E. Gianotti, L. Marchese, H. Tsuji, H. Hattori, Res. Chem. Intermed. 25 (1999) 77.
[16] H. Knözinger, S. Huber, J. Chem. Soc. Faraday Trans. 94 (1998) 2095.
[17] S. Coluccia, L. Marchese, G. Martra, Microporous Mesoporous Mater. 30 (1999) 43.
[18] C. Otero Areán, A.A. Tsyganenko, E.E. Platero, E. Garrone, A. Zecchina, Angew. Chem. Int. Ed. Engl. 37 (1998) 3161.
[19] A.M. Ferrari, P. Ugliengo, E. Garrone, J. Chem. Phys. 105 (1996) 4129.
[20] A.M. Ferrari, K.M. Neyman, N. Rösch, J. Phys. Chem. B 101 (1997) 9292.
[21] A. Zecchina, C. Otero Areán, G. Turnes Palomino, F. Geobaldo, C. Lamberti, G. Spoto, S. Bordiga, Phys. Chem. Chem. Phys. 1 (1999) 1649.
[22] D.A. Seanor, C.H. Amberg, J. Chem. Phys. 42 (1965) 2967.
[23] N.S. Hush, M.L. Williams, J. Mol. Spectrosc. 50 (1974) 349.
[24] E.E. Platero, D. Scarano, G. Spoto, A. Zecchina, Faraday Discuss. Chem. Soc. 80 (1985) 183.
[25] Y.F. Shepelev, A.A. Anderson, Y.I. Smolin, Zeolites 10 (1990) 61;
D.H. Olson, Zeolites 15 (1995) 439.

[26] S. Bordiga, E. Garrone, C. Lamberti, A. Zecchina, C. Otero Areán, V.B. Kazansky, L.M. Kustov, J. Chem. Soc. Faraday Trans. 90 (1994) 3367.
[27] Y. Okamoto, M. Ogawa, A. Maezawa, T. Imanaka, J. Catal. 112 (1988) 427.
[28] M. Huang, A. Adnot, S. Kaliaguine, J. Catal. 137 (1992) 322.
[29] J.C. Lavalley, Catal. Today 27 (1996) 377.
[30] G. Busca, V. Lorenzelli, Mater. Chem. 7 (1982) 89.
[31] L. Bertsch, H.W. Habgood, J. Phys. Chem. 67 (1963) 1621.
[32] M. Förster, M. Schumann, J. Chem. Soc. Faraday Trans. 85 (1989) 1149.
[33] C. Morterra, G. Cerrato, C. Emanuel, Mater. Chem. Phys. 29 (1991) 447.
[34] R.T. Sanderson, Chemical Bonds and Bond Energy, Academic Press, New York, 1976.
[35] M. Huang, S. Kaliaguine, J. Chem. Soc. Faraday Trans. 88 (1992) 1327.